Identification of a Suppressor of the *Dictyostelium* Profilin-minus Phenotype as a CD36/LIMP-II Homologue

Iakowos Karakesisoglou,* Klaus-Peter Janssen,* Ludwig Eichinger,* Angelika A. Noegel,‡ and Michael Schleicher*

*A.-Butenandt-Institut für Zellbiologie, Ludwig-Maximilians-Universität, 80336 München, Germany; and ‡Institut für Biochemie I, Universität zu Köln, 50931 Köln, Germany

Abstract. Profilin is an ubiquitous G-actin binding protein in eukaryotic cells. Lack of both profilin isoforms in *Dictyostelium discoideum* resulted in impaired cytokinesis and an arrest in development. A restriction enzyme–mediated integration approach was applied to profilin-minus cells to identify suppressor mutants for the developmental phenotype. A mutant with wild-type–like development and restored cytokinesis was isolated. The gene affected was found to code for an integral membrane glycoprotein of a predicted size of 88 kD containing two transmembrane domains, one at the NH_2 terminus and the other at the COOH terminus. It is homologous to mammalian CD36/LIMP-II and represents the first member of this family in *D. discoideum*, therefore the name DdLIMP is proposed. Targeted disruption of the *lmpA* gene in the profilin-minus background also rescued the mutant phenotype. Immunofluorescence revealed a localization in vesicles and ringlike structures on the cell surface. Partially purified DdLIMP bound specifically to PIP_2 in sedimentation and gel filtration assays. A direct interaction between DdLIMP and profilin could not be detected, and it is unclear how far upstream in a regulatory cascade DdLIMP might be positioned. However, the PIP_2 binding of DdLIMP points towards a function via the phosphatidylinositol pathway, a major regulator of profilin.

Key words: cytoskeleton • LIMP-II • CD36 • profilin-suppressor • phosphatidylinositides

THE actin cytoskeleton has been well established as the driving force for ameboid movement. It is also involved in many cellular processes like cytokinesis, phagocytosis, and macropinocytosis. The eukaryotic organism *Dictyostelium discoideum* is a convenient model system to study the cytoskeleton of nonmuscle cells because it has a haploid genome and can easily be used for molecular genetics. Upon starvation, the amebas undergo a simple developmental cycle that involves aggregation and differentiation, and is completed by formation of fruiting bodies carrying mature spores. Bacteria are the major food source of wild-type amebas, and a very efficient mechanism has evolved for the uptake of particles. Phagocytosis depends on the actomyosin machinery and on actin-binding proteins (Noegel and Luna, 1995; Aubry et al., 1997). The same holds true for the uptake of fluid by laboratory strains, which apparently occurs mainly by macropinocytosis in liquid medium (Hacker et al., 1997). Actin-based vesicular transport along the endosomal and lysosomal pathways has been well characterized (Temesvari et al., 1996). Ingested material from clathrin-coated pinosomes or clathrin-independent macropinosomes (>0.2 μm in diameter) enters acidic, lysosomal-like vesicles (Aubry et al., 1993), is degraded subsequently by hydrolytic enzymes, and transported to larger, nonacidic postlysosomes (Padh et al., 1993). The transport from lysosomes to postlysosomes as well as the following exocytosis has been shown to require the actin cytoskeleton (Rauchenberger et al., 1997).

Many of the described cellular events involve rapid reorganization of the actin cytoskeleton, which can be accomplished by fragmentation of existing filaments and subsequent elongation or polymerization of new actin filaments from a pool of G-actin. *D. discoideum* contains ~175 μM of total actin (Haugwitz et al., 1994), which would be polymerized almost completely under the ionic conditions of the cytosol, like in most eukaryotic cells. However, only 40% of the total actin is present as F-actin in unstimulated *Dictyostelium* cells.

I. Karakesisoglou and K.-P. Janssen contributed equally to this work.

I. Karakesisoglou's present address is Howard Hughes Medical Institute, Department of Molecular Genetics, Cell Biology, Biochemistry, and Molecular Biology, The University of Chicago, Chicago, IL 60637.

Address correspondence to Dr. Michael Schleicher, A.-Butenandt-Institut für Zellbiologie, Ludwig-Maximilians-Universität, Schillerstr. 42, 80336 München, Germany. Tel.: 49-89-5996-876. Fax: 49-89-5996-882. E-mail: schleicher@bio.med.uni-muenchen.de

Profilin was initially identified as the major G-actin sequestering protein (Carlsson et al., 1977), but is now known to have a far more complex influence on actin polymerization (Carlier and Pantaloni, 1997). Furthermore, this small ubiquitous protein has been shown to interact with actin-related proteins (Machesky et al., 1994) and proteins harboring proline-rich motifs like VASP (Reinhard et al., 1995). Its regulation by membrane phospholipids like PIP_2 or its precursor PIP has been described extensively in vitro (Lassing and Lindberg, 1985; Goldschmidt-Clermont et al., 1990). In the yeast *Saccharomyces cerevisiae*, the subcellular localization of profilin has been shown to be controlled by phosphoinositide metabolism in vivo (Ostrander et al., 1995). Depletion of plasma membrane PIP_2 levels resulted in a reversible translocation of profilin from the membrane to the cytosol. However, the cellular functions of profilin at the interface of the cytoskeleton and signal transduction are far from being understood (Sohn and Goldschmidt-Clermont, 1994).

Genetic studies in the fission yeast, *Schizosaccharomyces pombe*, suggest that profilin (*cdc3*) is an essential gene involved in regulating actin distribution in all phases of the cell cycle (Balasubramanian et al., 1994; Chang et al., 1996). *Drosophila* profilin is encoded by the essential gene *chickadee*, and analysis of the phenotype of viable mutant alleles revealed defects in bristle formation and oogenesis that were ascribed to disturbed actin organization (Cooley et al., 1992; Verheyen and Cooley, 1994; Manseau et al., 1996). Profilin seems to be indispensable for the development of multicellular organisms. This has further been underlined by the fact that profilin-deficient mice were not viable and died at early stages of development (Witke, W., A.H. Sharpe, and D.J. Kwiatkowski. 1993. The American Society for Cell Biology. 33rd annual meeting. *Mol. Biol. Cell.* 4:149a).

To gain insight into the in vivo functions of profilin in the ameboid eukaryote *Dictyostelium*, we have constructed mutants lacking both profilin isoforms by molecular genetics (Haugwitz et al., 1994). The profilin-minus mutant showed a severe and complex phenotype: single cells were up to 10 times larger than wild-type cells, F-actin content increased, motility decreased, and development ceased at early culmination. Profilin-minus cells were impaired in cytokinesis and formed multinucleated cells that grew on surfaces but could not withstand the shearing forces in shaking culture.

To investigate regulatory events upstream of profilin, we created suppressor mutants of the profilin-minus phenotype with a restriction enzyme–mediated integration (REMI)[1] approach. One mutant with rescued developmental phenotype was analyzed, and a single gene disruption had occurred in a gene coding for an integral membrane glycoprotein with homology to the mammalian CD36/LIMP-II family (LIMP-II: lysosomal integral membrane protein; Calvo et al., 1995).

This gene family is evolutionally conserved, and contains cell adhesion and lipid receptors at the cell surface as well as lysosomal membrane proteins. They share a common topology: one membrane spanning region located at the NH_2 terminus and another one the COOH terminus. CD36 was first isolated from human blood platelets (Tandon et al., 1989). Since then, it was shown to be expressed in other cell types, such as monocytes or adipocytes (Greenwalt et al., 1992). Moreover, a vast body of knowledge has been acquired regarding its function as a cell surface receptor with multiple ligands including: extracellular matrix proteins (Asch et al., 1993), modified lipoproteins (Endemann et al., 1993), long chain fatty acids (Baillie et al., 1996), and anionic phospholipids (Ryeom et al., 1996). The related class B scavenger receptor SR-BI shares this lipid receptor function, and has been shown recently by a knockout approach to be the long-sought receptor for high density lipoprotein in rodents (Rigotti et al., 1997). The human homologue of SR-BI, called CLA-1 (CD36-, LIMP-II-Analogous; Calvo and Vega, 1993), may have very similar physiological properties (Murao et al., 1997). Most proteins of the CD36/LIMP-II gene family are localized at the plasma membrane, like the founding member CD36, SR-BI, or CLA-1, whereas LIMP-II is found in vesicles of lysosomal origin (Vega et al., 1991). The function of LIMP-II is still unknown. However, it has been suggested to be a receptor involved in the transport of small molecules to the cytoplasm (Vega et al., 1991).

This is the first report of a CD36/LIMP-II/CLA-1 homologue in *D. discoideum*, and because its vesicular localization closely resembles the situation found for LIMP-II of human or rat origin, the name DdLIMP is proposed. The disruption of the gene either by insertional mutagenesis or by homologous recombination rescues the profilin-minus phenotype. Thus, DdLIMP might belong to an unraveled regulatory cascade upstream of profilin.

Materials and Methods

Cells and Reagents

D. discoideum wild-type strain AX2 and mutant strains were cultivated at 21°C, either on standard medium agar plates with *Klebsiella aerogenes* (Williams and Newell, 1976) or axenically in liquid nutrient medium (Claviez et al., 1982) in shaking suspension at 150 rpm or submerged in plastic culture dishes. All reagents were purchased from Sigma Chemical Co., if not stated otherwise. Antibodies against α-L-fucosidase (mAb 173-185-1) and coronin (mAb 176-3D-6) were kindly provided by Dr. G. Gerisch (Max-Planck-Institut for Biochemistry, Martinsried, Germany), and anti-vacuolin antibody (221-1-1) was provided by Dr. M. Maniak (MPI for Biochemistry, Martinsried, Germany). The hybridoma cell line ACTI that produces an mAb against *D. discoideum* actin (Simpson et al., 1984) was purchased from the American Type Culture Collection. Antibody against murine β-COP (mAb E5A3) was a gift from Dr. T. Kreis (Geneva, Switzerland). A cDNA library from HS2205 (De Lozanne and Spudich, 1987) growth phase cells was provided by Dr. R. Gräf (A.-Butenandt-Institut für Zellbiologie, Munich, Germany).

Molecular Cloning of the Disrupted Gene lmpA

Standard techniques were used for cloning, transformation, and screening (Sambrook et al., 1989). The REMI of plasmid DNA (Kuspa and Loomis, 1992) was performed on the *D. discoideum* mutant strain pII/Ia2 that lacks both profilin isoforms (Haugwitz et al., 1994). 10 μg of BamHI lin-

1. *Abbreviations used in this paper:* DAPI, 4,6-diamidino-2-phenylindole; ICAM, intercellular cell adhesion molecules; LIMP, lysosomal integral membrane protein; PC, phosphatidylcholine; PI, phosphatidylinositol; PS, phosphatidylserine; RB, REMI BamHI mutant; REMI, restriction enzyme–mediated integration.

earized plasmid pUCBsrΔBam (Adachi et al., 1994) along with 4 U DpnII were used for electroporation of 5×10^7 profilin-minus cells essentially as previously described (Haugwitz et al., 1994). The transformants were selected with 4 μg/ml of blasticidin S (ICN Biochemicals Inc.) for 10 d, and cloned on *K. aerogenes* by spreader dilutions. About 4,000 primary transformants from several transformations were tested, and six independent colonies showing a rescued fruiting body formation were isolated; one of them (RB2) was chosen for further analysis.

The integrated plasmid along with 2.6 kb of flanking genomic DNA was excised with ClaI, and the 7.2-kb DNA piece was cloned in *Escherichia coli.* An EcoRI fragment of 2.5 kb and shorter fragments of 2.0 and 1.1 kb generated by treatment with exonuclease III (Erase-a-Base; Stratagene) were subcloned in pUC19 (Yanisch-Perron et al., 1985). The fragments were sequenced with the chain termination dideoxy method (Sanger et al., 1977) using uni, reverse, and sequence specific primers. The isolated genomic sequence of the disrupted gene *lmpA* had a size of ~1.2 kb, it contained the 3′ end of the coding region but lacked the 5′ end. Therefore, a λExCell cDNA library was screened as described previously (Doering et al., 1991).

For screening, a 0.8-kb PCR fragment close to the known 5′ end of the genomic sequence was used and labeled with [α-^{32}P]dATP with the Prime-It random primer kit (Stratagene). From one positive clone the cDNA insert was amplified by PCR using primers of the λExCell flanking regions, cloned into pUC19, and sequenced. The isolated cDNA had a size of ~1.6 kb, contained the 5′ end, and overlapped with the 5′ region of the originally isolated ClaI fragment. To exclude possible errors resulting from PCR amplification of the λExCell cDNA clone, the sequence was confirmed with independently amplified and cloned PCR products. Using genomic DNA as a template, the 5′ region of the gene was amplified, cloned in pUC19 vector, and two independent clones were sequenced several times from both sides to obtain sequence information on the single intron.

For the targeted homologous recombination the following was performed: the first 0.62-kb of the 5′ region of the *lmpA* gene starting with the ATG and including the intron, was amplified by PCR on genomic DNA; and inserted into the pUCBsrΔBam vector via XbaI and BamHI sites. The correct insertion of the genomic fragment was determined by DNA sequencing. Control transformations were carried out with the pUCBsrΔBam vector without insert. Transformations of profilin-minus cells with this vector were performed as described by Haugwitz et al. (1994) and selection was performed as stated above.

Immunofluorescence Microscopy

For immunofluorescence studies, cells were allowed to attach to coverslips for 30 min in liquid nutrient medium, washed with Soerensen phosphate buffer, fixed with cold methanol (10 min), air dried, labeled and mounted as previously described (de Hostos et al., 1991). In case of α-L-fucosidase, cells were washed and starved for 6 h in Soerensen phosphate buffer before fixation. Secondary antibodies used for immunofluorescence included goat anti–mouse IgG and goat anti–rabbit IgG coupled to fluorescein or Cy3 (Dianova). The mounted cells were observed in an Axiophot microscope (Carl Zeiss). For counting nuclei, methanol-fixed cells were stained for 1 h with 0.5 μg/ml of 4,6-diamidino-2-phenylindole (DAPI; Sigma Chemical Co.) in PBS. The cells were washed in DAPI-free buffer, rinsed in distilled water, and mounted. Standard immunofluorescence preparations were viewed on an inverted microscope (Leica DM IRBE; Leica GmbH) with an 100× objective. Images were acquired using the Leica TCS NT confocal imaging system, transferred to a personal computer (Power Macintosh 8500/180), and further analyzed using the National Institutes of Health image public domain software and Adobe Photoshop 4.0.

Partial Purification of DdLIMP

Axenically grown log-phase AX2 cells were harvested, washed in Soerensen buffer, resuspended in homogenization buffer (30 mM Tris/HCl, 4 mM EGTA, 2 mM DTT, 30% sucrose, 5 mM benzamidine, 0.5 mM PMSF, 2 mM EDTA, 0.25% protease inhibitor cocktail, pH 8.0), and opened with a Parr bomb. The ruptured cells were further separated in cytosol and membrane fractions by centrifugation at 100,000 *g* for 1 h. By immunoblots, DdLIMP was found to be quantitatively localized in the pellet. The membranes were solubilized with 0.2% (final concentration) Triton X-100 for 60 min at 4°C. The material was subsequently centrifuged at 1,000 *g* for 5 min to remove particles and subjected to anion exchange chromatography on a DEAE column (DE52; Whatman Inc.) equilibrated with DEAE buffer (10 mM Tris/HCl, 1 mM EGTA, 1 mM DTT, 0.02% NaN_3, 1 mM benzamidine, 0.5 mM PMSF, 0.2% Triton X-100, pH 8.0). Bound proteins were eluted with a linear salt gradient (0–400 mM NaCl in DEAE buffer). DdLIMP eluted at a conductivity between 4 and 8 mS/cm. Fractions containing DdLIMP were pooled, dialyzed against ConA buffer (20 mM Tris/HCl, 50 mM NaCl, 1 mM $MnCl_2$, 1 mM $CaCl_2$, pH 8.0) containing 0.1% Triton X-100, and loaded onto a 2.6 × 5 cm ConA–Sepharose column (Pharmacia Biotech, Inc.) equilibrated in ConA buffer. The column was washed extensively with ConA buffer without detergent, and bound proteins were eluted stepwise with 20, 100, and 500 mM of methyl-α-D-mannose in ConA buffer without detergent. If necessary, the DdLIMP containing fractions were further purified on gel filtration columns (Sephacryl S300; Pharmacia), equilibrated in IEDANBP buffer (see below). We were able to obtain 1.1 mg of DdLIMP starting from 35 g of total membrane pellets (wet weight).

Sedimentation Assay for PIP_2 Binding

The sedimentation assay was accomplished as described (Touhara et al., 1995) with minor modifications. Partially purified DdLIMP was incubated with IEDAN buffer (control) or with phospholipids for 30 min on ice in a total volume of 150 μl. After centrifugation at 100,000 *g* for 20 min at 4°C, 50 μl from the top of the supernatant was removed and stored on ice and the rest of the supernatant was discarded. The pellets were washed once with 150 μl buffer, centrifuged at 100,000 *g* for 10 min, and resuspended in 150 μl buffer. Supernatants and pellets were analyzed by SDS-PAGE followed by Coomassie blue staining or immunoblotting. All assays were carried out in the presence of 1 mM $CaCl_2$ and the PIP_2 was quantitatively sedimented under these conditions according to Flanagan et al. (1997).

Gel Filtration Assay for Phospholipid Binding

DdLIMP-containing fractions were incubated 1:1 (vol/vol) with phospholipids or buffer (control) for 15 min on ice, centrifuged at 6,000 *g* for 10 min to remove aggregates, and 50 μl of the supernatant was immediately loaded on a Superose 6 PC 3.2/30 column (Smart System; Pharmacia Biotech, Inc.) at 4°C. The column was equilibrated in IEDANBP buffer (10 mM imidazol, 1 mM EGTA, 1 mM DTT, 0.02% NaN_3, 200 mM NaCl, 1 mM benzamidine, 0.5 mM PMSF, pH 7.6), and the flow rate was 40 μl/min. Fractions of 60 μl were collected and subjected to SDS-PAGE and Coomassie blue staining, or immunoblotting. Size calibration was carried out using ferritin (450 kD), catalase (240 kD), aldolase (158 kD), BSA (68 kD), and chymotrypsinogen (25 kD) as standard. To rule out a possible influence of Ca^{2+} on the protein–phospholipid interaction, all gel filtration assays were repeated in the presence of 1 mM Ca^{2+}. No significant variation was seen when duplicate experiments from both conditions were compared. Evaluation was done with the Smart Manager software package for OS/2.

Miscellaneous Methods

Preparation of DNA and RNA for Southern and Northern blot analyses was performed according to Noegel et al. (1985). SDS-PAGE (Laemmli, 1970) and immunoblotting (Towbin et al., 1979) followed standard procedures. Secondary antibodies used included: goat anti–mouse IgG and goat anti–rabbit IgG coupled to horseradish peroxidase (Dianova). The bound secondary antibodies were visualized with the enhanced chemiluminescence method (Nycomed Amersham). Determination of protein concentration was done according to Lowry et al. (1951) with BSA as a standard. Rabbit actin was prepared from skeletal muscle according to Spudich and Watt (1971). Recombinant and native *Dictyostelium* profilin were purified as described by Haugwitz et al. (1991). Polyclonal antisera 3416 and 3417 against DdLIMP were raised by immunizing rabbits (Eurogentec) with a bacterially expressed polypeptide comprising the COOH-terminal half of DdLIMP, starting at amino acid 390. The recombinant protein carrying an NH_2-terminal 6× His-tag was expressed in *E. coli* M15 cells using a pQE32 vector (Qiagen GmbH) and purified by Ni^{2+}-NTA affinity chromatography (Qiagen GmbH). Compilation of DNA or protein sequences was done with the UWGCG program (University of Wisconsin Genetics Computer Group; Devereux et al., 1984). Searches for similarities to other protein sequences were done with the BLAST program (Altschul et al., 1990) using the combined nonredundant entries of the Brookhaven Protein Data Bank, Swiss-Prot, PIR, and GenBank at the NCBI. Phylogenetic analysis was carried out with the program package PHYLYP (Felsenstein, 1989).

Results

Suppression of the Profilin-minus Phenotype after REMI Mutagenesis

The REMI technique, first described by Schiestl and Petes (1991), is a powerful method for tagging and cloning novel genes in model systems like *D. discoideum* (Kuspa and Loomis, 1992), *Candida albicans* (Brown et al., 1996), *Ustilago maydis* (Boelker et al., 1995), or in the vertebrate *Xenopus* (Kroll and Amaya, 1996). It has been used successfully to identify suppressors of developmental mutants in *D. discoideum* (Bear et al., 1998), and we applied it with the aim of isolating suppressor mutants for the profilin-minus phenotype. After 10 d of selective pressure the transformants were plated on *K. aerogenes* plates.

Six colonies (RB1–RB6: REMI BamHI) were found to develop normally, whereas the development of the profilin-minus cells was always arrested at the finger stage. Southern analysis showed that RB1–RB4 and RB5–RB6, respectively, had the same restriction pattern. If one assumes that they share the same insertion and multiple independent insertions took place, then the screen would be near saturation, in accordance with earlier suppressor screens with the REMI method (Shaulsky et al., 1996).

One clone (RB2) was chosen for further analysis; the flanking regions of the other strains have not been determined. Determination of the number of nuclei showed that the prominent cytokinesis defect of the profilin-minus cells, resulting in the frequent appearance of giant multinucleated cells, was also suppressed in the RB2 mutant (Fig. 1). However, the growth defects of profilin-minus cells were not restored. On bacterial lawn as well as in shaking culture at 120 rpm, RB2 had about the same growth rate as its parent strain pII/Ia2. Interestingly, the RB2 mutant seemed to be less prone to physical damage by shaking than the profilin-minus cells. Immunofluorescence studies showed that the broad F-actin rim frequently found in profilin-minus cells was not present in the RB2 strain. The F-actin distribution was indistinguishable from wild-type. Southern analysis of ClaI-digested genomic DNA from RB2, using a blasticidin S probe, showed a band of 7.2 kb in the REMI mutant. This band represents the plasmid used for mutagenesis with flanking sequences.

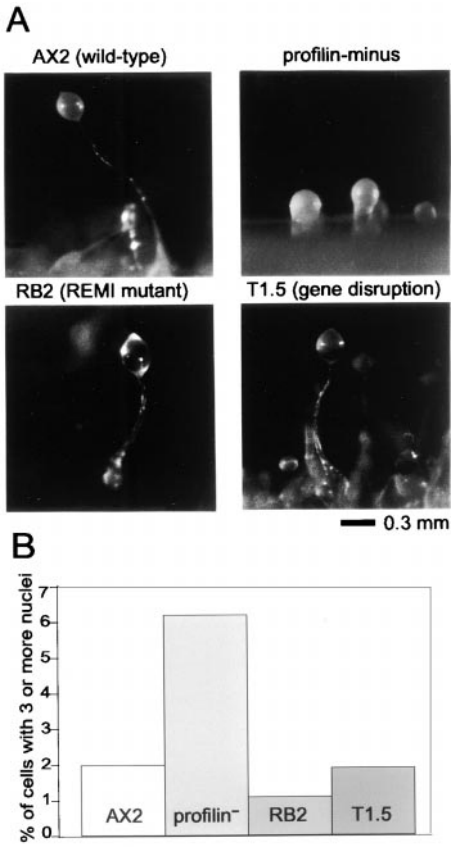

Figure 1. (A) Late development in wild-type cells and suppressor mutants. The cells were grown on *K. aerogenes* lawns and pictures were taken after 4 d. The wild-type strain AX2 shows normal fruiting bodies (top left), whereas the profilin-minus cells are arrested in their development at the onset of culmination (top right). In the REMI clone, RB2, the gene *lmpA* was disrupted and the mutant was found to show wild-type–like development (bottom left). Homologous recombination of *lmpA* resulted in the same suppressor phenotype (clone T1.5, bottom right). (B) The cytokinesis defect of profilin-minus cells is suppressed in the REMI clone RB2 and in the gene disruption mutant T1.5. Cells were grown in shaking culture at 120 rpm for several days, transferred to coverslips, fixed and stained with DAPI, and the number of nuclei per cell was counted. Giant multinucleated (>10 nuclei) cells were frequently found in the profilin-minus strain (total cell number $n = 570$), but not in the wild-type ($n = 200$). The RB2 strain ($n = 400$) as well as T1.5 ($n = 660$) showed a rescued cytokinesis.

lmpA Encodes a Protein with Homology to Lysosomal Integral Membrane Proteins

The pUCBsrΔBam plasmid together with 2.6 kb of flanking genomic sequence were recovered from the RB2 strain and subjected to sequence analysis. Two open reading frames were found. One had a size of 1.176 kb and was disrupted by the pUCBsrΔBam vector at a DpnII restriction site; the second had a size of 0.6 kb and showed the opposite orientation. Both open reading frames were separated by a sequence whose A/T composition is typical for intergenic DNA in the *Dictyostelium* genome. Due to sequence homology with mammalian LIMP-II, the gene and the encoded polypeptide were named *lmpA* and DdLIMP, respectively. The coding region of *lmpA* lacked the ATG start codon but contained a TAA stop codon, the most frequently found termination codon in *D. discoideum* (Sharp and Devine, 1989). Screening of a cDNA library resulted in the isolation of a cDNA clone with a size of ~1.6 kb that lacked the 3′ region of the gene but contained the ATG start codon. The cDNA and the genomic sequence overlapped by ~400 bp (Fig. 2 A). With primers derived from the completed coding sequence, PCR was carried out on AX2 genomic DNA to confirm the results from the cDNA sequencing reactions. In addition, a single 98-bp intron was found near the 5′ end of the coding sequence.

Examination of the deduced amino acid sequence of DdLIMP revealed a polypeptide with a length of 779 amino acids, a calculated molecular mass of 87.8 kD, and an isoelectric point of 4.4. A hydropathy profile according to the method of Kyte and Doolittle (1982) suggests two

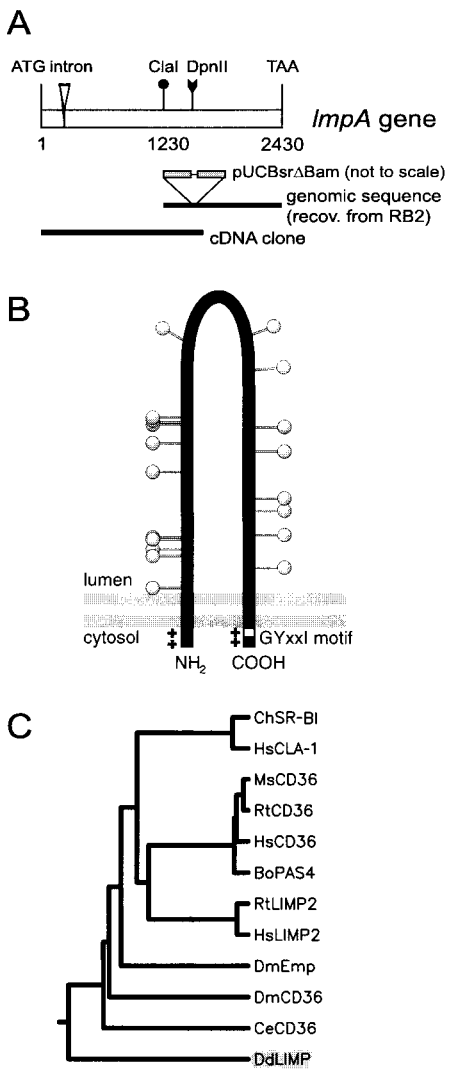

Figure 2. (A) Schematic representation of the *lmpA* gene. The ClaI restriction site, the DpnII site where the REMI vector integrated, and the single intron are indicated. The partial sequence recovered by isolation of the REMI vector with flanking sequences is shown below, together with the isolated partial cDNA clone, both overlapping by 0.4 kb. This sequence has been deposited in GenBank/EMBL/DDBJ under accession number AF124329. (B) Two transmembrane helices are strongly predicted for DdLIMP, with both termini residing at the cytoplasmic side. The schematic representation shows the likely intravesicular orientation of DdLIMP. Putative carbohydrate sidechains are represented by balls and sticks, and their spatial arrangement reflects the spacing of the predicted *N*-glycosylation sites along the primary sequence. The consensus lysosomal target motif is shown as an open box near the COOH terminus and the positive charge clusters are indicated. (C) Phylogenetic comparison of DdLIMP with homologous proteins of higher eukaryotes. The phylogenetic tree was computed using the PHYLYP program package, according to the least squares and Fitch-Margoliash method. The sequences used and their GenBank/EMBL/DDBJ accession numbers are the following: ChSR-BI, Chinese hamster scavenger receptor (A53920); HsCLA-1, human CD36/LIMPII analogous (A48528); MsCD36, mouse CD36 (L23108); RtCD36, rat fatty acid binding/transport protein (A47402); HsCD36, human CD36 (A54870); BoPAS4, bovine PAS-4 coding sequence (D45364); RtLIMP2, rat lysosomal integral membrane protein (JH0241); HsLIMP2, human lysosomal integral membrane protein (A56525); DmEmp, *Drosophila melanogaster* epithelial membrane protein (S38957); DmCD36, *D. melanogaster* croquemort (Z31583); CeCD36, *Caenorhabditis elegans* CD36-homologous protein (Q11124); and DdLIMP, *D. discoideum* (AF124329).

hydrophobic regions, one at the NH_2 terminus and one at the COOH terminus. The length of the apolar segment at the NH_2 terminus (24 amino acids) and the charge distribution in the flanking hydrophilic stretches suggest that this constitutes a signal anchor rather than a cleaved signal (Wahlberg and Spiess, 1997). In contrast, cleaved signal sequences have shorter apolar segments (7–15 residues; von Heijne, 1986). In the case of *Dictyostelium* ponticulin, a protein reported to have a cleaved signal sequence, the hydrophobic segment contains only 13 residues (Hitt et al., 1994). Rat LIMP-II, which is a mammalian homologue of DdLIMP was shown to contain an uncleaved signal peptide as well (Vega et al., 1991). There are 19 putative consensus sites for *N*-glycosylation present, and all of them are located in between the hydrophobic stretches (Fig. 2 B).

A comparison with the most recent databases using the BLASTP program (Altschul et al., 1990) revealed that DdLIMP was a novel *D. discoideum* protein related to LIMP-II of human and rat origin. Proteins of the LIMP-II class belong to the CD36, CLA-1, and LIMP-II gene family comprising single polypeptide membrane glycoproteins of apparently ubiquitous distribution in vertebrates and arthropods. As calculated with the program GAP (GCG program package), DdLIMP showed 35% similarity and 24% identity to rat LIMP-II, and 37% similarity and 25% identity to human CD36. There is a stretch of particular homology at the NH_2-terminal side (between the NH_2 terminus and amino acid 160), followed by several insertions only found in DdLIMP, which renders this protein the largest member of the family thus far. A recently identified structural domain common to all known members of the CD36/LIMP-II family, the CLESH-1 motif (Crombie and Silverstein, 1998), is located in this NH_2-terminal region (amino acids 101–149 in DdLIMP, corresponding to amino acids 85–133 in CD36 from humans). Two out of three blocks of this motif are well conserved in DdLIMP. A second homologous stretch with several breaks spans the region between amino acid 640 and the COOH terminus. There is a tyrosine-based lysosomal sorting motif **GYQAI** (Hunziker and Geuze, 1996) at a consensus position in the COOH-terminal bona fide cytosolic tail. Interestingly, this motif is only found in vertebrate proteins of the LAMP 1 family (lysosome-associated membrane protein; Honing and Hunziker, 1995), that show otherwise no significant sequence homology to DdLIMP. Mammalian LIMP-II lacks any tyrosine residues in this region and has a di-leucine sorting motif (Ogata and Fukuda, 1994; Sandoval et al., 1994).

Protein sequences of typical members of the CD36/LIMP-II/CLA-1 family from different species were aligned and used for a phylogenetic comparison using the program PHYLYP (Fig. 2 C; Felsenstein, 1989). DdLIMP is located at the bottom of the tree corresponding to the assumed evolutionary origin of *Dictyostelium* (after yeasts but be-

fore the metazoan radiation; Loomis and Smith, 1995). A BLASTP search with DdLIMP as query in the completed *S. cerevisiae* genome database (Stanford, CA) yielded no significant homologous sequences, making DdLIMP the most divergent member of this family.

Southern blot analysis of AX2 genomic DNA digested with various restriction enzymes indicated that *lmpA* is a single gene in the *Dictyostelium* genome, and no obvious cross-reacting bands were detectable under conditions of high stringency. To test for the existence of related sequences, the Southern blots were reprobed at low stringency (30% formamide). Only in one out of seven restriction digests that were tested, was an additional, lower size band observed. By Northern hybridization analysis a transcript of 3.5 kb could be detected (see Fig. 8 C), which is in agreement with the size of the complete *lmpA* coding sequence with an additional poly-A tail. However, a smaller additional transcript of 1.4 kb was observed in some cases. It is not clear whether the smaller transcript occurs because of a cross-reaction of the probe or arises from post-transcriptional processing. Interestingly, for both of the mammalian *lmpA* homologues CD36 and LIMP-II, two or more transcripts have been demonstrated (Abumrad et al., 1993; Calvo et al., 1995). The *lmpA* transcript is present at about equal amounts during all stages of the *Dictyostelium* development (not shown). The *lmpA* mRNA is not altered in the profilin-minus cells as compared to wild-type RNA (not shown). Northern analysis of the REMI mutant RB2 revealed a complete absence of the 3.5-kb transcript. However, a larger faint band of ~8 kb hybridized with the full-length *lmpA* probe (not shown). This large transcript is most probably generated at the endogenous *lmpA* start of transcription and contains the integrated REMI vector.

A polyclonal antiserum was raised by immunizing rabbits with the recombinant COOH-terminal half of DdLIMP. It recognized a single band of ~120 kD in Western blots of AX2 homogenates, and after centrifugation at 100,000 *g* the signal was almost exclusively found in the membranous pellet (Fig. 3). From quantitative immunoblots, one can estimate that DdLIMP has a cellular molarity of 0.5 μM, and constitutes ~0.1% of total membrane protein. The band was unchanged under nonreducing conditions. The size of the band exceeds the calculated molecular mass of 87.8 kD, suggesting a posttranslational modification. DdLIMP bound to the lectin ConA and could be eluted with α-D-mannose, which also points towards modification by *N*-glycosylation. The same band was observed in the profilin-minus strain, but was clearly absent from the REMI mutant RB2. Truncated forms of DdLIMP were not detected in the RB2 strain by the polyclonal antiserum. DdLIMP could not be extracted from the membrane pellet with buffer containing 0.5 M NaCl, but was solubilized with Triton X-100 (not shown), a typical behavior of integral membrane proteins. Taken together, these results suggest the following model: DdLIMP is an integral membrane protein, both the NH_2 and the COOH terminus are cytosolic, whereas the major part of the protein in between the two membrane spanning regions is presumably highly *N*-glycosylated and intravesicular. Similar hairpin-like structures have also been proposed for CD36 and LIMP-II (Vega et al., 1991; Abumrad et al., 1993).

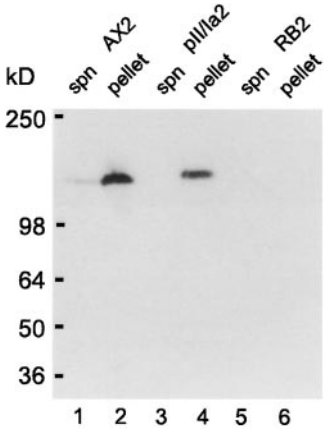

Figure 3. The polyclonal antiserum recognizes a single band for DdLIMP in the 100,000 *g* pellet. Cells from wild-type (lanes 1 and 2), profilin-minus cells (lanes 3 and 4), and the REMI mutant strain RB2 (lanes 5 and 6) were disrupted and the cell homogenates centrifuged for 1 h at 100,000 *g*. Aliquots of supernatants (spn) and pellets were subjected to immunoblotting and stained with anti-DdLIMP polyclonal antiserum 3417. The same blot was probed with mAb ACT1 to test for equal loading in all lanes (not shown).

DdLIMP Localizes to Vesicles and Larger Ringlike Structures

Immunofluorescence studies on the distribution of DdLIMP in AX2 cells showed that the majority of the protein localized to small vesicles (<0.5 μm) of varying size (Fig. 4 A). A particular membrane staining was not observed. However, it cannot be excluded from our data that part of the signal was located at the plasma membrane. This would not be surprising in the light of membrane recycling events occurring from postlysosomes. The same localization could be observed in the profilin-minus cells (not shown), whereas the DdLIMP staining was completely absent in the REMI mutant RB2 (Fig. 4 A). DdLIMP was not only found in vesicles, but it also localized to punctated rings surrounding larger vesicular structures (diam: 2.1 ± 0.6 μm, $n = 21$). These larger fluorescent rings corresponded to phase-opaque vesicles (Fig. 4 B). Double staining with an mAb against the lysosomal enzyme α-L-fucosidase was carried out using confocal microscopy (not shown). This protein, found in a major population of lysosomes, is developmentally regulated. Therefore, colocalization studies were conducted with cells after 6 h of starvation. In control experiments, it was shown that the DdLIMP localization pattern was not changed during this developmental stage. Surprisingly, it was found that there was no colocalization of both proteins.

To further investigate the nature of the DdLIMP-positive structures, double staining experiments with an heterologous antibody against the COPI coatomer protein, β-COP, were carried out. It was found that there was a substantial colocalization in the punctated rings, but not in the smaller vesicles (Fig. 5 A). β-COP plays a role in the early stages of the secretory pathway, as well as in early to late endosomal transfer (Whitney et al., 1995).

Double-labeling experiments with coronin, a protein found at phagocytically active cell projections known as crowns, revealed only minor colocalization (Fig. 5 B). However, in some cases, a double labeling of ringlike structures was observed. Essentially, the same was observed in double labeling experiments with vacuolin, a

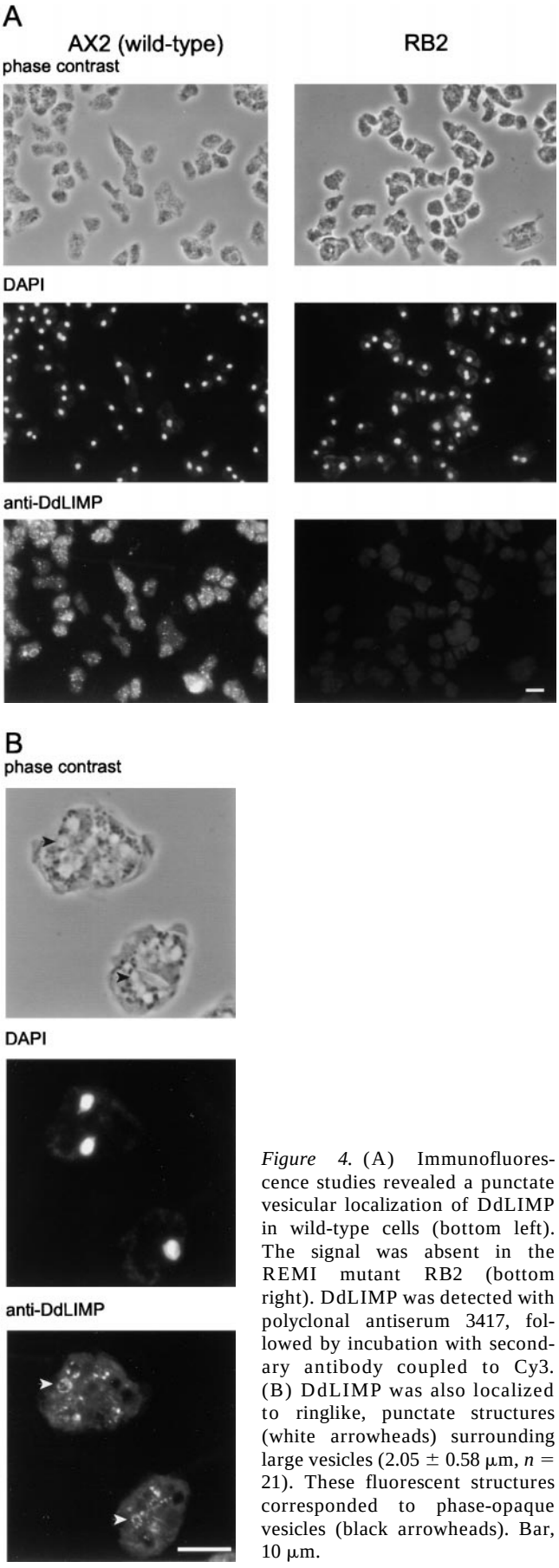

Figure 4. (A) Immunofluorescence studies revealed a punctate vesicular localization of DdLIMP in wild-type cells (bottom left). The signal was absent in the REMI mutant RB2 (bottom right). DdLIMP was detected with polyclonal antiserum 3417, followed by incubation with secondary antibody coupled to Cy3. (B) DdLIMP was also localized to ringlike, punctate structures (white arrowheads) surrounding large vesicles (2.05 ± 0.58 μm, n = 21). These fluorescent structures corresponded to phase-opaque vesicles (black arrowheads). Bar, 10 μm.

marker for postlysosomes (Rauchenberger et al., 1997); only a small subpopulation of the punctated rings was both vacuolin- and DdLIMP-positive. These findings indicate a presence of DdLIMP in the endosomal pathway. In fact, some of the large punctate rings may be macropinosomes.

In Vitro Binding Assays

DdLIMP was partially purified from *D. discoideum* AX2 cells by conventional chromatography and used for in vitro binding assays. It was first tested whether DdLIMP was able to directly interact with profilin. This was done by immunoprecipitation of cell homogenates with mAbs for profilin I and II (Haugwitz et al., 1991), or anti-DdLIMP polyclonal antiserum, and subsequent immunostaining. No coprecipitation of DdLIMP and either of the profilins was observed; the same result was obtained when profilin was precipitated by poly(L-proline) (Tanaka and Shibata, 1985) coupled to agarose beads (not shown). Recombinant profilin I and II were incubated with DdLIMP or rabbit actin, treated with the chemical cross-linking agent EDC as described by Haugwitz et al. (1991), and analyzed by SDS-PAGE and immunoblotting. The control clearly showed cross-linking of both profilins to actin, whereas no profilin–DdLIMP complexes were observed in the treatment group (not shown).

Since actin is known to play a role in vesicle transport along the endolysosomal pathway in *Dictyostelium* (Hacker et al., 1997; Rauchenberger et al., 1997), one might assume an interaction of the membrane protein DdLIMP with the microfilament system. To test this possibility, DdLIMP was incubated with rabbit actin under polymerizing conditions on ice for 1 h and the polymerized actin filaments were pelleted by centrifugation at 100,000 *g* for 30 min. No DdLIMP was detected in the pellets by analysis with SDS-PAGE and immunoblotting (not shown).

DdLIMP Binds to Inositol Phospholipids

To test the interaction with phospholipids, we incubated partially purified DdLIMP (Fig. 6 A, arrow) with PIP_2 in micellar form and centrifuged the mixture at 100,000 *g*. DdLIMP alone was found to be soluble, and was sedimented only in the presence of PIP_2, whereas the contaminating peptide p60 (Fig. 6 A, open arrowhead) stayed in the supernatant. To exclude that the interaction was only due to nonspecific interaction of the transmembrane domains of DdLIMP with the hydrophobic part of the phospholipid, control experiments with cationic phosphatidylcholine (PC) were carried out (Fig. 6 B), and no interaction was found. Phosphatidylserine (PS), like PIP_2, belongs to the class of anionic phospholipids, and has been described as a ligand for mammalian CD36 (Rigotti et al., 1995; Ryeom et al., 1996). Liposomes solely composed of negatively charged PS were able to sediment more DdLIMP than PC liposomes. However, there was still significantly less binding as compared to PIP_2 (Fig. 6 C). DdLIMP also bound PIP_2 in mixed liposomes in the presence of a fivefold excess of PC (Fig. 6, B and D). Under these conditions, a significant amount (~50%) of DdLIMP was sedimented by the mixed liposomes. About the same affinity was found for PC/PI(4)P mixtures, but significantly less sedimentation was observed with PC/PS liposomes (Fig. 6

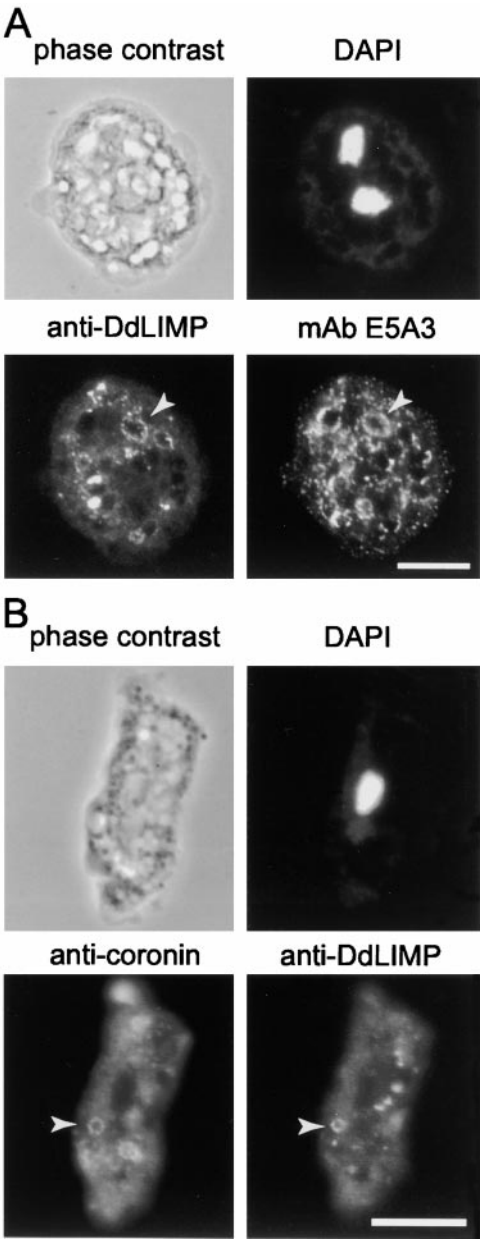

Figure 5. (A) Double staining with antibodies against the murine coatomer protein, β-COP, and DdLIMP is shown. AX2 cells were incubated with polyclonal antiserum 3417 (DdLIMP) and mAb E5A3 (β-COP) and subsequently with secondary antibody coupled to fluorescein and Cy3, respectively. (B) Colocalization of the actin-binding protein, coronin, and DdLIMP is shown. AX2 cells were double labeled with polyclonal antiserum 3417 (DdLIMP) and mAb 176-3D-6 (coronin), and incubated as described above. Arrowheads point to a ringlike structure at the dorsal face of the cell. Bar, 10 μm.

D). Since the major part of the DdLIMP protein is proposed to localize to the lumen of endolysosomal compartments of putative low pH, the pH dependence of the protein–phospholipid interaction was also tested. It was found that the binding characteristics, at pH 5.0, were comparable to the assays done at pH 7.6. In contrast, binding was abolished at pH 9.0.

In gel filtration assays, DdLIMP bound to PIP_2 micelles but not to control liposomes. A Superose 6 column was used with the Smart System that allowed the application of very small samples and had excellent detection capabilities. Calibration of the column with molecular mass standards (Fig. 7 C) indicated a high reproducibility of the retention volume. When DdLIMP was applied to the column in the absence of phospholipid, it eluted at 1.51 ± 0.02 ml (mean ± SD for three experiments), which corresponds to a molecular mass of 240 kD (Fig. 7 A, filled arrow). The contaminating p60 eluted at 1.74 ml (Fig. 7 A, arrowhead), corresponding to 50 kD. The discrepancy in the observed elution of DdLIMP (240 kD) and the relative mass calculated from the electrophoretic behavior in reducing gels (120 kD) might reflect a dimerization of DdLIMP, which has been observed for the higher eukaryote homologues SR-BI (Landschulz et al., 1996), CD36 (Thorne et al., 1997), and FAT (Ibrahimi et al., 1996), but could also arise from unusual elution behavior and the presence of tightly bound detergent molecules. However, the elution behavior did not change when the protein preparation was incubated with PC (Fig. 7 D) or PS (not shown). Upon addition of PIP_2 micelles, which are reported to have a relative molecular mass of 93 kD (aggregation number 82) in aqueous solutions (Sugiura, 1981), the elution of DdLIMP shifted to 1.42 ml (440 kD), whereas the p60 peak was essentially unchanged at 1.72 ml (60 kD). The same was observed with a phospholipid mixture from biological origin (brain phospholipids, Folch fraction), which contains 50% PS and 10% inositol phospholipids.

Confirmation of REMI Results by Targeted Homologous Recombination

To make sure that the observed rescue phenotype of the REMI mutant RB2 was really due to the disruption of the *lmpA* gene, homologous recombination was carried out on the profilin-minus strain. The gene disruption vector included a 620-bp genomic DNA of the *lmpA* gene together with a blasticidin S resistance cassette. The transformants were selected for 10 d, cloned, and screened for a wild-type–like phenotype. In control transformations with the vector alone, no suppressor colonies were observed.

One clone (T1.5) with phenotypically normal fruiting bodies and wild-type–like cytokinesis in shaking culture was chosen for further analysis. Immunofluorescence studies showed a decrease in the DdLIMP signal and densitometric scanning of immunoblots revealed that DdLIMP was still present, but reduced by a factor of two (Fig. 8 D). About 50 mutants that were unable to form fruiting bodies were picked randomly and analyzed as nonsuppressor controls. None of them had an altered DdLIMP signal, as judged by immunoblotting. Southern hybridization assays with genomic DNA from the T1.5 clone confirmed a disruption of the *lmpA* gene (Fig. 8 A). A radiolabeled probe specific for the resistance cassette detected only one band (Fig. 8 B), indicating a single integration of the vector in the genome. The integration of the bsr vector restored the complete *lmpA* open reading frame, but apparently dis-

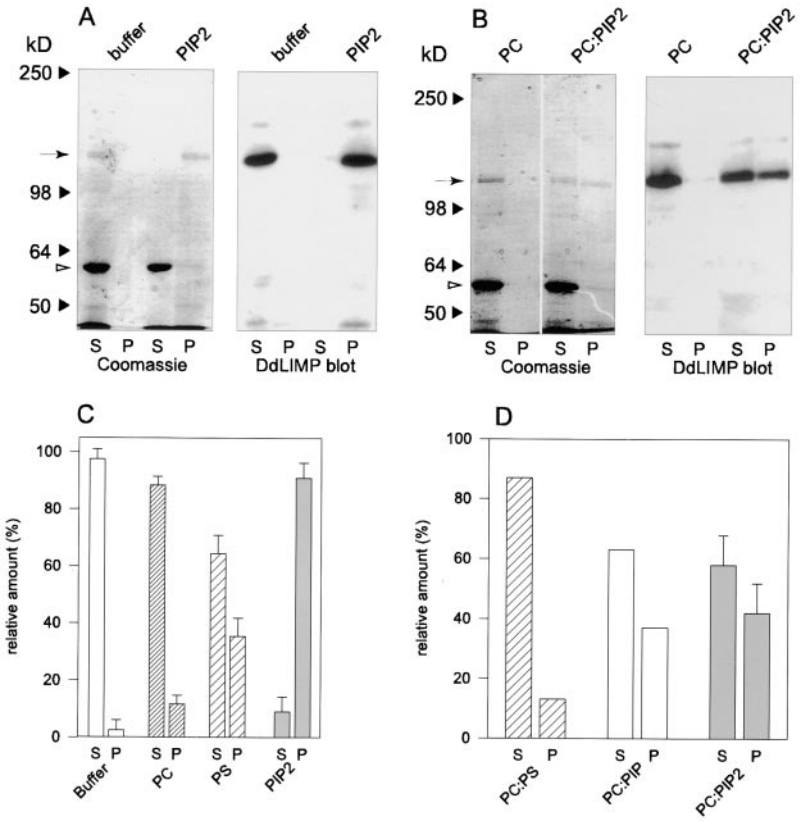

Figure 6. DdLIMP can be sedimented at 100,000 *g* by PIP_2 micelles and mixed PC/PIP_2 liposomes. (A) Partially purified DdLIMP was incubated with IEDAN buffer (control), or with PIP_2 micelles (final concentration 0.5 mg/ml) for 30 min on ice. After centrifugation at 100,000 *g* for 20 min, supernatants were removed, pellets washed once, and resuspended in the original volume before analysis by SDS-PAGE. Proteins were labeled by Coomassie staining or with antiserum 3417 after immunoblotting. The contaminating p60 (open arrowhead) stays soluble even in the presence of phospholipid. (B) DdLIMP does not bind to control PC vesicles, but mixed liposomes (PC/PIP_2 at a 5:1 ratio) can also pellet a substantial amount of DdLIMP. (C) The highest amount of DdLIMP is sedimented with PIP_2, there is only minute binding to PC, and moderate binding to the anionic phospholipid PS. Quantification by densitometry, shown as mean ± SD of three independent experiments. (D) The same holds true for experiments with mixed liposomes. DdLIMP binds equally well to liposomes containing PC/$PI(4,5)P_2$ and PC/PI(4)P, but only minor sedimentation was observed for PC/PS mixtures (all liposomes mixed at 5:1 ratio).

placed the endogenous ATG and the 5′ untranslated sequence (Fig. 8 E), resulting in the appearance of a second larger transcript (Fig. 8 C). The partial reduction of the DdLIMP concentration resulted in a very similar, but not identical phenotype as compared to the original REMI clone RB2. The gene disruption mutant had a reduced cell size (~20% smaller) as compared to RB2. Even though both suppressor strains were able to form phenotypically normal fruiting bodies, they were not able to produce viable, detergent-resistant spores. This was tested by treatment of fully developed aggregates with 0.5% Triton X-100 and subsequent plating on bacteria. Wild-type spores easily withstood that treatment, whereas in the suppressor strains no colonies were observed. Sorocarps from both suppressor strains were completely devoid of wild-type–like oval encapsulated spores as judged by light microscopy.

Gene Disruption of lmpA in a Wild-Type Background

To gain further evidence on the role of DdLIMP, a *lmpA*-minus strain was created by homologous recombination in the wild-type strain AX2. For this purpose, the gene disruption vector containing a 620-bp homologous fragment, from the 5′ end of the *lmpA* gene (described above), was slightly modified to prevent restoration of the complete open reading frame by recombination of endogenous and vector *lmpA* sequence. The vector was digested with the restriction enzyme AccI (that cuts once in the *lmpA* coding sequence), treated with S1-nuclease, and religated. By this treatment, a 2-bp deletion was introduced in the *lmpA* open reading frame, thus giving rise to a frameshift mutation.

AX2 was transformed with the ΔAccI vector and the transformants were selected for 10 d with blasticidin S. 600 clones were picked randomly and analyzed by immunofluorescence and immunoblotting for the absence of the DdLIMP signal. Only one clone (T2.25) was found to have an obviously reduced amount of DdLIMP in immunoblots and a very weak staining in immunofluorescence, pointing towards a homologous recombination event. Southern analysis of genomic DNA revealed a shift in the *lmpA* bands for T2.25. In the case of strain T1.17, a nonhomologous control transformant, the endogenous *lmpA* bands were unchanged and additional bands occurred that corresponded to the vector. PCR analysis on genomic DNA using vector and gene specific primers further confirmed a homologous integration for T2.25 and a nonspecific integration for T1.17. Northern analysis with a full-length *lmpA* probe revealed a transcript indistinguishable from wild-type in T1.17.

In the case of T2.25, the 3.5-kb mRNA was reduced twofold and a second, larger transcript had appeared, comparable to the full-circle clone T1.5 (Fig. 8 C). The gene disruption strain T2.25 showed normal cytokinesis and developed into wild-type–like fruiting bodies. However, the number and size of fruiting bodies was reduced as compared to the wild-type. The sorocarps contained viable, detergent-resistant spores, but their number was strongly decreased. In comparison to the wild-type strain, AX2, the number of round uncoated spores in the sorocarp was increased by a factor of five (as judged by light

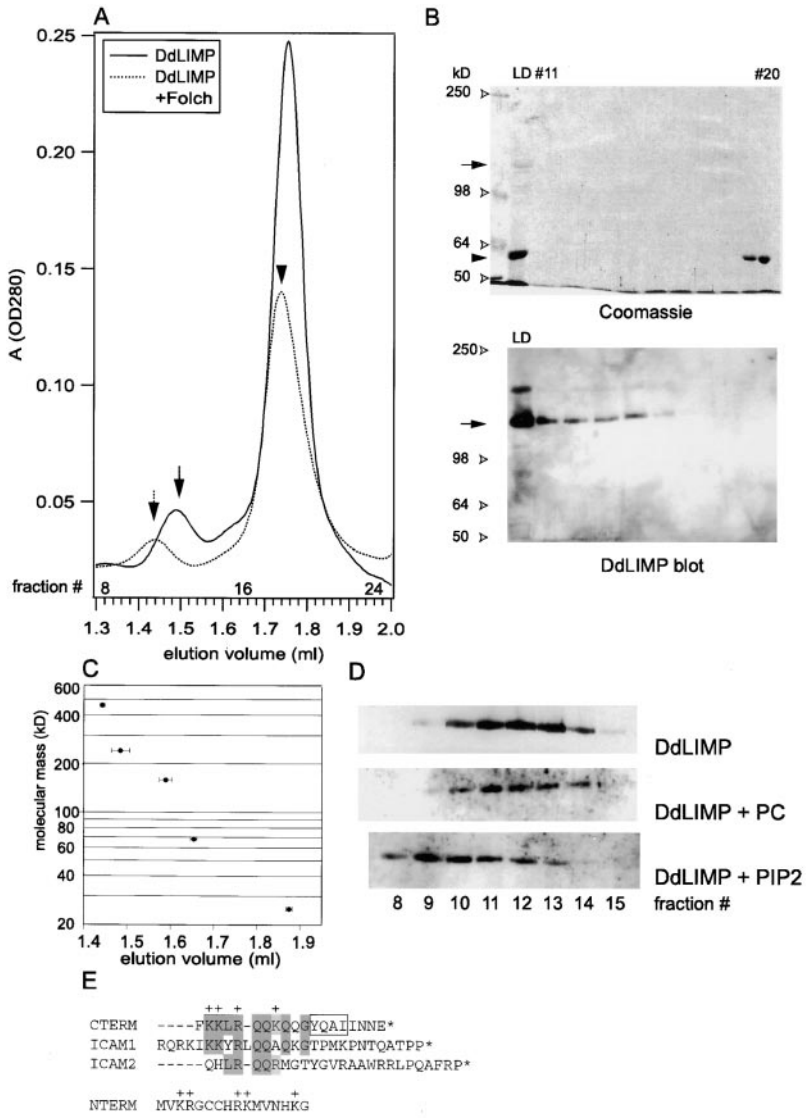

Figure 7. Gel filtration assay for PIP_2 binding. DdLIMP-containing fractions were incubated with buffer (control), or various phospholipids, and subjected to gel filtration chromatography on a Superose 6 column (Smart System). (A) Chromatogram showing the UV absorption of the collected fractions. DdLIMP eluted at 1.50 ml, whereas the contaminating peptide p60 (filled arrowhead in B) eluted at a volume of 1.74 ml. Upon incubation (1:1 vol/vol) with brain phospholipid extracts (Folch fraction; Sigma Chemical Co.) at a final concentration of 1.25 mg/ml, the elution of DdLIMP shifted to 1.43 ml (arrows in A denote the shifted elution peaks). The p60 elution was not significantly changed, it stayed within the experimental variation at 1.72 ml. The amplitude of the second run is lower due to dilution of the proteins with the phospholipid solution. (B) This was further confirmed by applying aliquots of the collected fractions to SDS-PAGE. Coomassie staining and immunoblotting identified the first peak as DdLIMP, the second as p60. (C) Calibration of the column was carried out with ferritin, aldolase, catalase, BSA, and chymotrypsinogen. (D) DdLIMP also bound to pure PIP_2. Shown are immunoblots of the corresponding experiments: the elution is shifted by two fractions in the presence of PIP_2, but not with PC or PS (not shown). All experiments were done in duplicate. (E) The otherwise unrelated human cell adhesion molecules ICAM-1 and ICAM-2 show similarities in their cytosolic COOH terminus to the corresponding region of DdLIMP (CTERM). The ICAMs have been shown to bind PIP_2 in this region, and the basic charges are thought to mediate the interaction. The sequences of the cytosolic tails (starting with the first cytosolic amino acid) have been aligned with CLUSTAL. The NH_2 terminus of DdLIMP (NTERM) is shown for comparison.

microscopy). The T2.25 strain had normal growth rates on bacteria, but showed greatly reduced growth in submersion culture. Furthermore, it was unable to withstand shearing forces in shaking culture at 150 rpm (Fig. 9). After 2 d in shaking culture, many small vesicle-like fragments appeared that might be due to extensive membrane shedding. The control strain T1.17 grew normally, although slightly slower than the wild-type under all conditions tested, and was not impaired in growth at 150 rpm. Similar to the full-circle clone T1.5, the cell size of T2.25 was reduced slightly, whereas the control strain T1.17 had a size distribution comparable to the wild-type.

Discussion

We have used the REMI approach to investigate regulatory cascades upstream of profilin by screening for suppressor mutants in profilin-minus *D. discoideum* cells. The disrupted gene *lmpA* was recovered from the mutant and coded for an integral membrane glycoprotein with PIP_2 binding activity, constituting the first reported *Dictyostelium* homologue of the CD36/LIMP-II/CLA-1 gene family. Targeted homologous recombination of *lmpA* in a profilin-minus background resulted in a similar suppressor phenotype.

DdLIMP Is a Dictyostelium Homologue of Mammalian LIMP-II

It has been shown that there are many high molecular weight, low pI, integral membrane glycoproteins in purified lysosomal membranes from *D. discoideum* (Temesvari et al., 1994). However, no LAMPs or LIMPs have been reported to date. DdLIMP showed significant homology to the CD36/LIMP-II/CLA-1 family of integral membrane proteins from mammalian or insect origin. The overall structural features appear to be quite well conserved evolutionarily, from the position of the two transmembrane domains to the glycosylation pattern. Apart from its function in cell adhesion and signal transduction

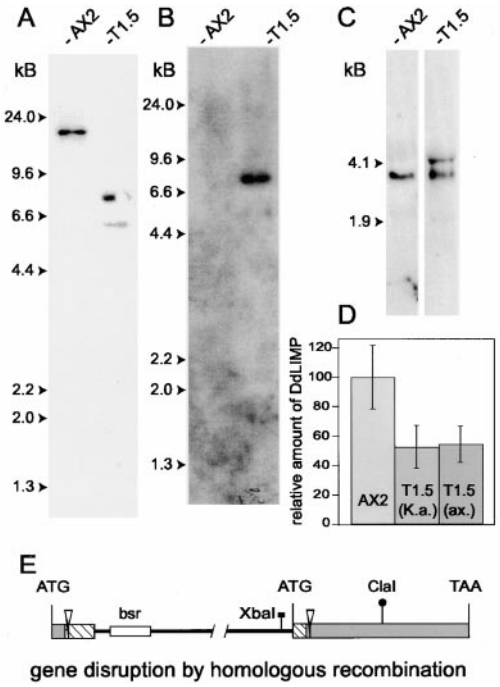

Figure 8. Southern blot analysis of the homologous recombination of *lmpA* in a profilin-minus background. Genomic DNA of wild-type cells and the gene disruption mutant T1.5 was digested with XbaI (A) or ClaI (B), and hybridized with a full-length *lmpA* probe (A), or a probe for the blasticidin resistance cassette (B). A restriction site for XbaI is introduced by the gene disruption vector, resulting in two bands in the mutant T1.5 (A). There is no ClaI site in the vector, and as expected only one fragment can be detected resulting from a single integration (B). (C) Northern blot hybridized with a full-length *lmpA* probe showing an additional transcript in the gene disruption mutant T1.5. (D) The concentration of DdLIMP is reduced by a factor of two in the gene disruption mutant T1.5. Cells grown on bacterial lawns (K.a.) or in axenic culture (ax.) were harvested, lysed, adjusted to equal protein concentration, and analyzed by densitometric scanning of immunoblots. Means and standard deviation for at least six independent experiments are shown. (E) Schematic representation of the expected result of the *lmpA* gene disruption by homologous recombination is shown. The *lmpA* portion included in the vector is shown cross-hatched. The endogenous sequence is shown in light gray.

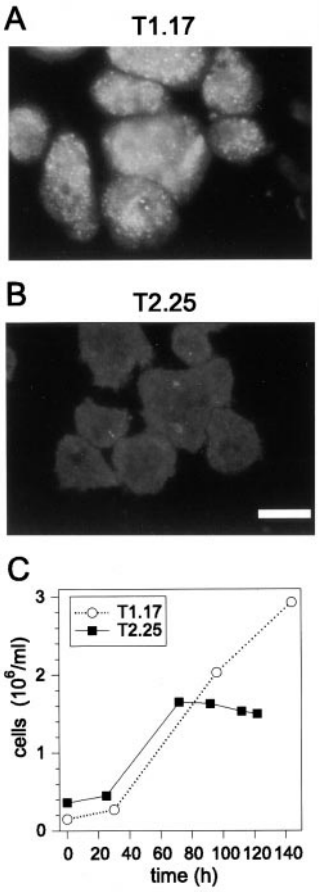

Figure 9. Gene disruption of *lmpA* in a wild-type background. Immunofluorescence staining with anti-DdLIMP antiserum of (A) the nonhomologous control transformant T1.17 and (B) the *lmpA* gene disruption clone T2.25. Bar, 10 μm. (C) Growth in shaking culture is impaired in the gene disruption clone T2.25, but not in the control transformant T1.17. Curves are representative experiments.

(Hirao et al., 1997), CD36 and other members of the gene family, notably the scavenger receptor SR-BI (Acton et al., 1996) and the CD36 homologue FAT from adipocytes (Ibrahimi et al., 1996), have been identified as lipid receptors that bind long-chain fatty acids (Abumrad et al., 1993; Baillie et al., 1996), PI, and PS (Rigotti et al., 1995; Ryeom et al., 1996). The adipose CD36 homologue FAT has been reported to exist as a homodimer and, possibly, as part of an oligomeric transport complex (Ibrahimi et al., 1996).

Since DdLIMP was localized on vesicles rather than at the plasma membrane, it bears more similarity to LIMP-II than to the other members of the CD36/LIMP-II/CLA-1 family shown to be cell surface molecules (Calvo et al., 1995). However, our immunofluorescence studies identified the DdLIMP-positive vesicles and the α-L-fucosidase–positive lysosomes as two different populations. According to Souza et al. (1997), there are two separate populations of lysosomes in *D. discoideum*, which are either acidic and glycosidase-rich or of more neutral pH and rich in cysteine proteases. Thus, DdLIMP may be localized in the cysteine protease-containing lysosome population. DdLIMP was also found in larger punctate ringlike structures (diam 2 ± 0.6 μm) that resemble macropinosomes (1.6 ± 0.3 μm; Hacker et al., 1997) or postlysosomes (>2 μm; Buczynski et al., 1997) that are reported to be less acidic than lysosomes (Cardelli et al., 1989).

An intriguing feature of DdLIMP is its apparent divergent lysosomal sorting motif. Mammalian LIMP-II shows a typical di-leucine type motif (Leu-Ile) in the short COOH-terminal tail that extends into the cytosol (Ogata and Fukuda, 1994; Sandoval et al., 1994), whereas the corresponding sequence in DdLIMP (**GY**QA**I**) more closely resembles the tyrosine-based signal of the LAMP1 type (**GY**QT**I**; Honing and Hunziker, 1995). Mammalian LIMP-II interacts with the recently identified nonclathrin AP-3 adaptor complex via its di-leucine signal (Honing et al., 1998). On the other hand, the proteins of the LAMP1 family have only one membrane-spanning domain and the sequences are unrelated to DdLIMP. The tyrosine motif is thought to act as a binding site for adaptor protein complexes (AP1 or AP2), and it has been shown to target LAMP1 to lysosomes (Honing et al., 1996), or plasma membrane proteins to endosomes (Ohno et al., 1995).

Even though PI lipids constitute only a small fraction of total lipids in the membranes of eukaryotic cells, they are

thought to play a pivotal role in vesicle transport, signal transduction, and cytoskeletal regulation. PIP_2 constitutes a central component in the polyphosphatidylinositide pathway by serving as a precursor to several inositol lipid second messengers and directly regulating protein localization and activity of many actin-binding proteins. In *Dictyostelium* endolysosomes, PIP_2 accounts for 9% of total lipids, as compared to 11% in the plasma membrane (Nolta et al., 1991).

Most of the many proteins described that bind to PIP_2 are cytosolic. Thus far, only two integral membrane proteins with PIP_2 binding activity have been described: the inward rectifier potassium channel from cardiac muscle (Huang et al., 1998) and the human intercellular cell adhesion molecules-1 and -2 (ICAM-1 and -2) (Heiska et al., 1998). None of the classical PIP_2-binding sequence motifs (e.g., the KxxxKxKK signature; Yu et al., 1992) can be found in DdLIMP. There is considerable heterogeneity in the primary sequence domains and structures that are reported to bind to inositol phospholipids (Janmey, 1995; Shaw, 1996). However, in all cases the interactions are mediated by positively charged amino acid residues on the protein and the negatively charged phosphate groups on the inositol headgroup. In addition to the electrostatic interactions, hydrophobic segments are thought to contribute to binding (Janmey and Stossel, 1989). Given the assumed membrane topology of DdLIMP and the localization of inositol phospholipids in the cytoplasmic leaflet of cellular membranes (Schroit and Zwaal, 1991), it is feasible that the short cytosolic tails of DdLIMP account for binding to the negatively charged inositol headgroup. ICAM-1, the first described cell adhesion molecule with PIP_2-binding activity, is an otherwise unrelated protein that has a relatively short (27 amino acid) COOH-terminal tail containing a high amount of positively charged residues. This tail is sufficient for phospholipid binding and induces interaction of ICAM-1 and ezrin (Heiska et al., 1998). Comparison of DdLIMP to ICAM-1 and ICAM-2 (both binding to PIP_2) shows a considerable degree of similarity in this region (Fig. 7 E), whereas ICAM-3, which does not bind to PIP_2, shares no significant similarities with DdLIMP.

How Could a Knockout of lmpA Possibly Rescue the Profilin-minus Phenotype?

Since disruption of the *lmpA* gene suppresses the profilin-minus phenotype there must be some interaction, direct or circumstantial, between the cytosolic actin-binding protein, profilin, and the integral membrane protein, DdLIMP. A direct binding of profilin to DdLIMP is unlikely, as judged from our own in vitro binding studies and the lack of polyproline stretches in DdLIMP, the most characteristic feature of recently found profilin-binding proteins like VASP (Reinhard et al., 1995), diaphanous from *Drosophila* (Castrillon and Wasserman, 1994), and p140mDia from mammals (Watanabe et al., 1997). In the fission yeast *S. pombe*, mutations in the essential gene *sop2* or in *arp3* were reported to rescue the temperature-sensitive lethality of a profilin mutant (Balasubramanian et al., 1996; McCollum et al., 1996). The gene product Sop2p shows homology to the β-transducin family and is thought to interact with a protein complex containing profilin, actin, and Arp3p. In *S. cerevisiae*, an interaction of profilin with the vesicular transport system responsible for exocytosis was found by identification of SEC3, a component of the exocyst protein complex, as a profilin synthetic lethal gene (Haarer et al., 1996). None of those bona fide profilin ligands or interacting partners bear similarity to the membrane proteins of the LIMP-II class.

Interestingly, unpublished observations (Cardelli, J., and M. Schleicher) showed that the profilin-minus mutant exhibited a strong defect in endocytosis, exocytosis, and the secretion of the lysosomal enzyme acid phosphatase. The vesicle transport defects are partially restored in both the original REMI mutant RB2 as well as the recapitulation strain T1.5. There are several lines of evidence supporting a connection between the signal transduction pathway, known as PI cycle, profilin, and actin-dependent vesicle transport during endocytosis or exocytosis. Knocking out the PI3-kinases in macrophages inhibited the completion of macropinocytosis and phagocytosis (Araki et al., 1996). Accordingly, the loss of the related kinases *DdPIK1* and *DdPIK2* in *Dictyostelium* amebas had severe defects in endocytosis, transport from lysosomes to postlysosomes, and the actin cytoskeleton (Buczynski et al., 1997).

Recently, human profilin has been shown to bind the lipid products of PI3-kinases with higher affinity than Ptd-Ins(4,5)P_2 (Lu et al., 1996). Apart from being a possible downstream target of the PI3-kinases in the endosomal pathway, there is a more direct evidence for an interaction of profilin with phagocytosis in *Dictyostelium*. It has been shown that actin and several actin-binding proteins are associated with phagocytic cups and early phagosomes (Boyles and Bainton, 1981; Furukawa and Fechheimer, 1994; Rezabek et al., 1997), and the same holds true for profilin (our unpublished observations). The uptake of fluid and particles by *D. discoideum* depended on the actin cytoskeleton (Maniak et al., 1995; Hacker et al., 1997). Also, it was shown recently that depolymerization of F-actin by cytochalasin A inhibited exocytosis (Rauchenberger et al., 1997). The fact that myosin I mutants exhibit defects in endocytosis, exocytosis, and secretion of lysosomal enzymes further underlines the tight linkage of the actin cytoskeleton to lysosome-related membrane events in *Dictyostelium* (Temesvari et al., 1996).

Profilin, like other cytoskeletal proteins (Janmey et al., 1992), binds with high affinity to the membrane phospholipid PIP_2 and to a lesser extent to its precursor PIP (Lassing and Lindberg, 1985). The phosphoinositide metabolism is proposed to be responsible for the partitioning of profilin between the plasma membrane and the cytosol (Ostrander et al., 1995), which is thought to be crucial for the regulation of the microfilament system. It has been proposed that a substantial fraction of total PIP_2 in the inner leaflet of the plasma membrane is bound by profilin (Goldschmidt-Clermont et al., 1990). Binding to profilin inhibits the hydrolysis of PIP_2 by phospholipase Cγ, and plays an important role in the polyphosphoinositide pathway, which has been reported to involve Rac-driven GTPase activity (Hartwig et al., 1995). The loss of profilin in ameba cells results in a severe and multiple phenotype (Haugwitz et al., 1994) that might be mediated not only by

the increased amount of F-actin, but also by an altered spectrum of phospholipids. This in turn acts on polyphosphoinositide-regulated actin-binding proteins. In the profilin-minus mutants, DdLIMP as a putative receptor or transporter of phosphatidylinositides would not be counterbalanced by the abundant PIP_2-binding protein profilin. A disruption of the gene that codes for the lipid carrier could compensate the loss of profilin and rescue most of the phenotypic changes.

We thank Dr. R. Gräf for providing a cDNA library; antibodies were provided by Dr. G. Gerisch and the late Dr. T. Kreis. We thank Dr. J. Cardelli (Department of Microbiology, Louisiana State University Medical Center, Shreveport, LA) for fruitful discussion and critical reading of the manuscript, and T. Zimmermann (Ludwig-Maximilians-University, München) for technical advice on confocal microscopy. We are also grateful to D. Rieger and M. Dietz for excellent technical assistance.

The work was supported by grants from the Deutsche Forschungsgemeinschaft to A.A. Noegel and M. Schleicher, and by funds from the Fonds der Chemischen Industrie and the Friedrich-Baur-Stiftung.

Received for publication 10 October 1998 and in revised form 8 December 1998.

References

Abumrad, N.A., M.R. El-Maghrabi, E. Amri, E. Lopez, and P.A. Grimaldi. 1993. Cloning of a rat adipocyte membrane protein implicated in binding or transport of long-chain fatty acids that is induced during preadipocyte differentiation. *J. Biol. Chem.* 268:17665–17668.

Acton, S., A. Rigotti, K.T. Landschulz, S. Xu, H.H. Hobbs, and M. Krieger. 1996. Identification of scavenger receptor SR-BI as a high density lipoprotein receptor. *Science.* 271:518–520.

Adachi, H., T. Hasebe, K. Yoshinaga, T. Ohta, and K. Sutoh. 1994. Isolation of *Dictyostelium discoideum* mutants by restriction enzyme-mediated integration of the blasticidin S resistance marker. *Biochem. Biophys. Res. Commun.* 205:1808–1814.

Altschul, S.F., W. Gish, W. Miller, E.W. Myers, and D.J. Lipman. 1990. Basic local alignment search tool. *J. Mol. Biol.* 215:403–410.

Araki, N., M.T. Johnson, and J.A. Swanson. 1996. A role for phosphoinositide 3-kinase in the completion of macropinocytosis and phagocytosis by macrophages. *J. Cell Biol.* 135:1249–1260.

Asch, A.S., I. Liu, F.M. Briccetti, J.W. Barnwell, F. Kwakye-Berko, A. Dokun, J. Goldberger, and M. Pernambuco. 1993. Analysis of CD36 binding domains: ligand specificity controlled by dephosphorylation of an ectodomain. *Science.* 262:1436–1440.

Aubry, L., G. Klein, J.L. Martiel, and M. Satre. 1993. Kinetics of endosomal pH evolution in *Dictyostelium discoideum* amoebae. Study by fluorescence spectroscopy. *J. Cell Sci.* 105:861–866.

Aubry, L., G. Klein, and M. Satre. 1997. Cytoskeletal dependence and modulation of endocytosis in *Dictyostelium discoideum* amoebae. *In* Dictyostelium: A Model System for Cell and Developmental Biology. Y. Maeda, K. Inouye, and I. Takeuchi, editors. Universal Academy Press, Inc., Tokyo, Japan. 65–74.

Baillie, A.G.S., C.T. Coburn, and N.A. Abumrad. 1996. Reversible binding of long-chain fatty acids to purified FAT, the adipose CD36 homolog. *J. Membr. Biol.* 153:75–81.

Balasubramanian, M.K., B.R. Hirani, J.D. Burke, and K.L. Gould. 1994. The *Schizosaccharomyces pombe cdc3+* gene encodes a profilin essential for cytokinesis. *J. Cell Biol.* 125:1289–1301.

Balasubramanian, M.K., A. Feoktistova, D. McCollum, and K.L. Gould. 1996. Fission yeast Sop2p: a novel and evolutionarily conserved protein that interacts with Arp3p and modulates profilin function. *EMBO (Eur. Mol. Biol. Organ.) J.* 15:6426–6437.

Bear, J.E., J.F. Rawls, and C.L. Saxe III. 1998. SCAR, a WASP-related protein, isolated as a suppressor of receptor defects in late *Dictyostelium* development. *J. Cell Biol.* 142:1325–1335.

Boelker, M., H.U. Bohnert, K.H. Braun, J. Gorl, and R. Kahmann. 1995. Tagging pathogenicity genes in *Ustilago maydis* by restriction enzyme-mediated integration (REMI). *Mol. Gen. Genet.* 248:547–552.

Boyles, J., and D.F. Bainton. 1981. Changes in plasma-membrane-associated filaments during endocytosis and exocytosis in polymorphonuclear leukocytes. *Cell.* 24:905–914.

Brown, D.H., I.V. Slobodkin, and C.A. Kumamoto. 1996. Stable transformation and regulated expression of an inducible reporter construct in *Candida albicans* using restriction enzyme-mediated integration. *Mol. Gen. Genet.* 251:75–80.

Buczynski, G., B. Grove, A. Nomura, M. Kleve, J. Bush, R.A. Firtel, and J. Cardelli. 1997. Inactivation of two *Dictyostelium discoideum* genes *DdPIK1* and *DdPIK2*, encoding proteins related to mammalian phosphatidylinositide 3-kinases, results in defects in endocytosis, lysosome to postlysosome transport, and actin cytoskeleton organization. *J. Cell Biol.* 136:1271–1286.

Calvo, D., and M.A. Vega. 1993. Identification, primary structure, and distribution of CLA-1, a novel member of the CD36/LIMPII gene family. *J. Biol. Chem.* 268:18929–18935.

Calvo, D., J. Dopazo, and M.A. Vega. 1995. The CD36, CLA-1 (CD36L1), and LIMPII (CD36L2) gene family: cellular distribution, chromosomal location, and genetic evolution. *Genomics.* 25:100–106.

Cardelli, J.A., J.M. Richardson, and D. Miears. 1989. Role of acidic intracellular compartments in the biosynthesis of *Dictyostelium* lysosomal enzymes: the weak bases ammonium chloride and chloroquine differentially affect proteolytic processing and sorting. *J. Biol. Chem.* 264:3454–3463.

Carlier, M.F., and D. Pantaloni. 1997. Control of actin dynamics in cell motility. *J. Mol. Biol.* 269:459–467.

Carlsson, L., L.E. Nystrom, I. Sundkvist, F. Markey, and U. Lindberg. 1977. Actin polymerizability is influenced by profilin, a low molecular weight protein in nonmuscle cells. *J. Mol. Biol.* 115:465–483.

Castrillon, D.H., and S.A. Wasserman. 1994. Diaphanous is required for cytokinesis in *Drosophila* and shares domains of similarity with the products of the limb deformity gene. *Development.* 120:3367–3377.

Chang, F., A. Woollard, and P. Nurse. 1996. Isolation and characterization of fission yeast mutants defective in the assembly and placement of the contractile actin ring. *J. Cell Sci.* 109:131–142.

Claviez, M., K. Pagh, H. Maruta, W. Baltes, P. Fisher, and G. Gerisch. 1982. Electron microscopic mapping of monoclonal antibodies on the tail region of *Dictyostelium* myosin. *EMBO (Eur. Mol. Biol. Organ.) J.* 1:1017–1022.

Cooley, L., E. Verheyen, and K. Ayers. 1992. *chickadee* encodes a profilin required for intercellular cytoplasm transport during *Drosophila* oogenesis. *Cell.* 69:173–184.

Crombie, R., and R. Silverstein. 1998. Lysosomal integral membrane protein II binds thrombospondin. *J. Biol. Chem.* 273:4855–4863.

de Hostos, E.L., B. Bradtke, F. Lottspeich, R. Guggenheim, and G. Gerisch. 1991. Coronin, an actin-binding protein of *Dictyostelium discoideum* localized to cell surface projections, has sequence similarities to G protein β subunits. *EMBO (Eur. Mol. Biol. Organ.) J.* 10:4097–4104.

De Lozanne, A., and J. Spudich. 1987. Disruption of the *Dictyostelium* myosin heavy chain gene by homologous recombination. *Science.* 236:1086–1091.

Devereux, J., P. Haeberli, and O. Smithies. 1984. A comprehensive set of sequence analysis programs for the VAX. *Nucleic. Acids Res.* 12:387–395.

Doering, V., M. Schleicher, and A.A. Noegel. 1991. *Dictyostelium* annexin VII (synexin). cDNA sequence and isolation of a gene disruption mutant. *J. Biol. Chem.* 266:17509–17515.

Endemann, G., L.W. Stanton, K.S. Madden, C.M. Bryant, R.T. White, and A.A. Protter. 1993. CD36 is a receptor for oxidized low density lipoprotein. *J. Biol. Chem.* 268:11811–11816.

Felsenstein, J. 1989. PHYLIP - Phylogeny Inference Package (Version 3.2). *Cladistics.* 5:164–166.

Flanagan, L.A., C.C. Cunningham, J. Chen, G.D. Prestwich, K.S. Kosik, and P.A. Janmey. 1997. The structure of divalent cation-induced aggregates of PIP_2 and their alteration by gelsolin and tau. *Biophys. J.* 73:1440–1447.

Furukawa, R., and M. Fechheimer. 1994. Differential localization of α-actinin and the 30 kD actin-bundling protein in the cleavage furrow, phagocytic cup, and contractile vacuole of *Dictyostelium discoideum*. *Cell Motil. Cytoskeleton.* 29:46–56.

Goldschmidt-Clermont, P.J., L.M. Machesky, J.J. Baldassare, and T.D. Pollard. 1990. The actin-binding protein profilin binds to PIP_2 and inhibits its hydrolysis by phospholipase C. *Science.* 247:1575–1578.

Greenwalt, D.M., R.H. Lipsky, C.F. Ockenhouse, H. Ikeda, N.N. Tandon, and G.A. Jamieson. 1992. Membrane glycoprotein CD36: a review of its roles in adherence, signal transduction, and transfusion medicine. *Blood.* 80:1105–1115.

Haarer, B.K., A. Corbett, Y. Kweon, A.S. Petzold, P. Silver, and S.S. Brown. 1996. SEC3 mutations are synthetically lethal with profilin mutations and cause defects in diploid-specific bud-site selection. *Genetics.* 144:495–510.

Hacker, U., R. Albrecht, and M. Maniak. 1997. Fluid-phase uptake by macropinocytosis in *Dictyostelium*. *J. Cell Sci.* 110:105–110.

Hartwig, J.H., G.M. Bokoch, C.L. Carpenter, P.A. Janmey, L.A. Taylor, A. Toker, and T.P. Stossel. 1995. Thrombin receptor ligation and activated rac uncap actin filament barbed ends through phosphoinositide synthesis in permeabilized human platelets. *Cell.* 82:643–653.

Haugwitz, M., A.A. Noegel, D. Rieger, F. Lottspeich, and M. Schleicher. 1991. *Dictyostelium discoideum* contains two profilin isoforms that differ in structure and function. *J. Cell Sci.* 100:481–489.

Haugwitz, M., A.A. Noegel, J. Karakesisoglou, and M. Schleicher. 1994. *Dictyostelium* amoeba that lack G-actin-sequestering profilins show defects in F-actin content, cytokinesis, and development. *Cell.* 79:303–314.

Heiska, L., K. Alfthan, M. Groenholm, P. Vilja, A. Vaheri, and O. Carpen. 1998. Association of ezrin with intercellular adhesion molecule-1 and -2 (ICAM-1 and ICAM-2). Regulation by phosphatidylinositol 4,5-bisphosphate. *J. Biol. Chem.* 273:21893–21900.

Hirao, A., I. Hamaguchi, T. Suda, and N. Yamaguchi. 1997. Translocation of the Csk homologous kinase (Chk/Hyl) controls activity of CD36-anchored Lyn tyrosine kinase in thrombin-stimulated platelets. *EMBO (Eur. Mol. Biol. Organ.) J.* 16:2342–2351.

Hitt, A.L., T.H. Lu, and E.J. Luna. 1994. Ponticulin is an atypical membrane protein. *J. Cell Biol.* 126:1421–1431.

Honing, S., and W. Hunziker. 1995. Cytoplasmic determinants involved in direct lysosomal sorting, endocytosis, and basolateral targeting of rat lgp120 (lamp-I) in MDCK cells. *J. Cell Biol.* 128:321–332.

Honing, S., J. Griffith, H.J. Geuze, and W. Hunziker. 1996. The tyrosine-based lysosomal targeting signal in lamp-1 mediates sorting into Golgi-derived clathrin-coated vesicles. *EMBO (Eur. Mol. Biol. Organ.) J.* 15:5230–5239.

Honing, S., I.V. Sandoval, and K. von Figura. 1998. A di-leucine-based motif in the cytoplasmic tail of LIMP-II and tyrosinase mediates selective binding of AP-3. *EMBO (Eur. Mol. Biol. Organ.) J.* 17:1304–1314.

Huang, C.-L., S. Feng, and D.W. Hilgemann. 1998. Direct activation of inward rectifier potassium channels by PIP_2 and its stabilization by Gβγ. *Nature.* 391:803–806.

Hunziker, W., and H.J. Geuze. 1996. Intracellular trafficking of lysosomal membrane proteins. *Bioessays.* 18:379–389.

Ibrahimi, A., Z. Sfeir, H. Magharaie, E. Amri, P. Grimaldi, and N.A. Abumrad. 1996. Expression of the CD36 homolog (FAT) in fibroblast cells: effects on fatty acid transport. *Proc. Natl. Acad. Sci. USA.* 93:2646–2651.

Janmey, P.A. 1995. Protein regulation by phosphatidylinositol lipids. *Chem. Biol.* 2:61–65.

Janmey, P.A., and T.P. Stossel. 1989. Gelsolin-polyphosphoinositide interaction. Full expression of gelsolin-inhibiting function by polyphosphoinositides in vesicular form and inactivation by dilution, aggregation, or masking of the inositol head group. *J. Biol. Chem.* 264:4825–4831.

Janmey, P.A., J. Lamb, P.G. Allen, and P.T. Matsudaira. 1992. Phosphoinositide-binding peptides derived from the sequences of gelsolin and villin. *J. Biol. Chem.* 267:11818–11823.

Kroll, K.L., and E. Amaya. 1996. Transgenic *Xenopus* embryos from sperm nuclear transplantation reveal FGF signaling requirement during gastrulation. *Development.* 122:3173–3183.

Kuspa, A., and W.F. Loomis. 1992. Tagging developmental genes in *Dictyostelium* by restriction enzyme-mediated integration of plasmid DNA. *Proc. Natl. Acad. Sci. USA.* 89:8803–8807.

Kyte, J., and R.F. Doolittle. 1982. A simple method for displaying the hydropathic character of a protein. *J. Mol. Biol.* 157:105–132.

Laemmli, U.K. 1970. Cleavage of structural proteins during assembly of the head of bacteriophage T_4. *Nature.* 227:680–685.

Landschulz, K.T., R.K. Pathak, A. Rigotti, M. Krieger, and H.H. Hobbs. 1996. Regulation of scavenger receptor, class B, type I, a high density lipoprotein receptor, in liver and steroidogenic tissues of the rat. *J. Clin. Invest.* 98:984–995.

Lassing, I., and U. Lindberg. 1985. Specific interaction between phosphatidylinositol 4,5-bisphosphate and profilactin. *Nature.* 314:472–474.

Loomis, W.F., and D.W. Smith. 1995. Consensus phylogeny of *Dictyostelium*. *Experientia.* 51:1110–1115.

Lowry, O.H., N.J. Rosebraugh, A.L. Farr, and R.J. Randall. 1951. Protein measurement with the Folin phenol reagent. *J. Biol. Chem.* 193:265–275.

Lu, P.J., W.R. Shieh, S.G. Rhee, H.L. Yin, and C.S. Chen. 1996. Lipid products of phosphoinositide 3-kinase bind human profilin with high affinity. *Biochemistry.* 35:14027–14034.

Machesky, L.M., S.J. Atkinson, C. Ampe, J. Vandekerckhove, and T.D. Pollard. 1994. Purification of a cortical complex containing two unconventional actins from *Acanthamoeba* by affinity chromatography on profilin–agarose. *J. Cell Biol.* 127:107–115.

Maniak, M., R. Rauchenberger, R. Albrecht, J. Murphy, and G. Gerisch. 1995. Coronin involved in phagocytosis: dynamics of particle induced relocalization visualized by a green fluorescent protein tag. *Cell.* 83:915–924.

Manseau, L., J. Calley, and H. Phan. 1996. Profilin is required for posterior patterning of the *Drosophila* oocyte. *Development.* 122:2109–2116.

McCollum, D., A. Feoktistova, M. Morphew, M. Balasubramanian, and K.L. Gould. 1996. The *Schizosaccharomyces pombe* actin-related protein, Arp3, is a component of the cortical actin cytoskeleton and interacts with profilin. *EMBO (Eur. Mol. Biol. Organ.) J.* 15:6438–6446.

Murao, K., V. Terpstra, S.R. Green, N. Kondratenko, D. Steinberg, and O. Quehenberger. 1997. Characterization of CLA-1, a human homologue of rodent scavenger receptor SR-BI, as a receptor for high density lipoprotein and apoptotic thymocytes. *J. Biol. Chem.* 272:17551–17557.

Noegel, A.A., and J.E. Luna. 1995. The *Dictyostelium* cytoskeleton. *Experientia.* 51:1135–1143.

Noegel, A.A., D.L. Welker, B.A. Metz, and K.L. Williams. 1985. Presence of nuclear associated plasmids in the lower eukaryote *Dictyostelium discoideum*. *J. Mol. Biol.* 185:447–450.

Nolta, K.V., H. Padh, and T.L. Steck. 1991. Acidosomes from *Dictyostelium*. *J. Biol. Chem.* 266:18318–18323.

Ogata, S., and M. Fukuda. 1994. Lysosomal targeting of limpII membrane glycoprotein requires a novel Leu-Ile motif at a particular position in its cytoplasmic tail. *J. Biol. Chem.* 269:5210–5217.

Ohno, H., J. Stewart, M.C. Fournier, H. Bosshart, I. Rhee, S. Miyatake, T. Saito, A. Gallusser, T. Kirchhausen, and J.S. Bonifacio. 1995. Interaction of tyrosine-based sorting signals with clathrin-associated proteins. *Science.* 269: 1872–1875.

Ostrander, D.B., J.A. Gorman, and G.M. Carman. 1995. Regulation of profilin localization in *Saccharomyces cerevisiae* by phosphoinositide metabolism. *J. Biol. Chem.* 270:27045–27050.

Padh, H., J. Ha, M. Lavasa, and T.L. Steck. 1993. A post-lysosomal compartment in *Dictyostelium discoideum*. *J. Biol. Chem.* 268:6742–6747.

Rauchenberger, R., U. Hacker, J. Murphy, J. Nieswoehner, and M. Maniak. 1997. Coronin and vacuolin identify consecutive stages of a late, actin-coated endocytic compartment in *Dictyostelium*. *Curr. Biol.* 7:215–218.

Reinhard, M., K. Giehl, K. Abel, C. Haffner, T. Jarchau, V. Hoppe, B.M. Jockusch, and U. Walter. 1995. The proline-rich focal adhesion and microfilament protein VASP is a ligand for profilins. *EMBO (Eur. Mol. Biol. Organ.) J.* 14:1583–1589.

Rezabek, B.L., J.M. Rodriguez-Paris, J.A. Cardelli, and C.P. Chia. 1997. Phagosomal proteins of *Dictyostelium discoideum*. *J. Eukaryot. Microbiol.* 44:284–292.

Rigotti, A., S.L. Acton, and M. Krieger. 1995. The class B scavenger receptors SR-BI and CD36 are receptors for anionic phospholipids. *J. Biol. Chem.* 270: 16221–16224.

Rigotti, A., B.L. Trigatti, M. Penman, H. Rayburn, J. Herz, and M. Krieger. 1997. A targeted mutation in the murine gene encoding the high density lipoprotein (HDL) receptor scavenger receptor class B type I reveals its key role in HDL metabolism. *Proc. Natl. Acad. Sci. USA.* 94:12610–12615.

Ryeom, S.W., R.L. Silverstein, A. Scotto, and J.R. Sparrow. 1996. Binding of anionic phospholipids to retinal pigment epithelium may be mediated by the scavenger receptor CD36. *J. Biol. Chem.* 271:20536–20539.

Sambrook, J., E.F. Fritsch, and T. Maniatis. 1989. Molecular Cloning. Cold Spring Harbor Laboratory Press, Cold Spring Harbor, NY. 1379 pp.

Sandoval, I.V., J.J. Arredondo, J. Alcalde, A. Gonzalez Noriega, J. Vandekerckhove, M.A. Jimenez, and M. Rico. 1994. The residues Leu(Ile)(475)-Ile(Leu,Val,Ala)(476), contained in the extended carboxyl cytoplasmic tail, are critical for targeting of the resident lysosomal membrane protein limpII to lysosomes. *J. Biol. Chem.* 269:6622–6631.

Sanger, F., S. Nicklen, and A.R. Coulson. 1977. DNA sequencing with chain-terminating inhibitors. *Proc. Natl. Acad. Sci. USA.* 74:5463–5467.

Schiestl, R.H., and T.D. Petes. 1991. Integration of DNA fragments by illegitimate recombination in *Saccharomyces cerevisiae*. *Proc. Natl. Acad. Sci. USA.* 88:7585–7589.

Schroit, A.J., and R.F.A. Zwaal. 1991. Transbilayer movement of phospholipids in red cell and platelet membranes. *Biochim. Biophys. Acta.* 1071:313–329.

Sharp, P.M., and K.M. Devine. 1989. Codon usage and gene expression level in *Dictyostelium discoideum* highly expressed genes do "prefer" optimal codons. *Nucleic Acids Res.* 17:5029–5039.

Shaulsky, G., R. Escalante, and W.F. Loomis. 1996. Developmental signal transduction pathways uncovered by genetic suppressors. *Proc. Natl. Acad. Sci. USA.* 93:15260–15265.

Shaw, G. 1996. The pleckstrin homology domain: an intriguing multifunctional protein module. *Bioessays.* 18:35–46.

Simpson, P.A., J.A. Spudich, and P. Parham. 1984. mAbs prepared against *Dictyostelium* actin: characterization and interactions with actin. *J. Cell Biol.* 99: 287–295.

Sohn, R.H., and P.J. Goldschmidt-Clermont. 1994. Profilin: at the crossroads of signal transduction and the actin cytoskeleton. *Bioessays.* 16:465–472.

Souza, G.M., D.P. Mehta, M. Lammertz, J. Rodriguez-Paris, R. Wu, J.A. Cardelli, and H.H. Freeze. 1997. *Dictyostelium* lysosomal proteins with different sugar modifications sort to functionally distinct compartments. *J. Cell Sci.* 110:2239–2248.

Spudich, J.A., and S. Watt. 1971. The regulation of rabbit skeletal muscle contraction. I. Biochemical studies of the interaction of the tropomyosin-troponin complex with actin and the proteolytic fragments of myosin. *J. Biol. Chem.* 246:4866–4871.

Sugiura, Y. 1981. Structure of molecular aggregates of 1-(3-*sn*-phosphatidyl)-L-*myo*-inositol 3,4-bisphosphate) in water. *Biochim. Biophys. Acta.* 641:148–159.

Tanaka, M., and H. Shibata. 1985. Poly(L-proline)-binding proteins from chick embryos are a profilin and a profilactin. *Eur. J. Biochem.* 151:291–297.

Tandon, N.N., R.H. Lipsky, W.H. Burgess, and G.A. Jamieson. 1989. Isolation and characterization of platelet glycoprotein IV (CD36). *J. Biol. Chem.* 264: 7570–7575.

Temesvari, L., J. Rodriguez-Paris, J. Bush, T.L. Steck, and J. Cardelli. 1994. Characterization of lysosomal membrane proteins of *Dictyostelium discoideum*. *J. Biol. Chem.* 269:25719–25727.

Temesvari, L.A., J.M. Bush, M.D. Peterson, K.D. Novak, M.A. Titus, and J.A. Cardelli. 1996. Examination of the endosomal and lysosomal pathways in *Dictyostelium discoideum* myosin I mutants. *J. Cell Sci.* 109:663–673.

Thorne, R.F., C.J. Meldrum, S.J. Harris, D.J. Dorahy, D.R. Shafren, M.C. Berndt, G.F. Burns, and P.G. Gibson. 1997. CD36 forms covalently associated dimers and multimers in platelets and transfected COS-7 cells. *Biochem. Biophys. Res. Commun.* 240:812–818.

Touhara, K., W.J. Koch, B.E. Hawes, and R.J. Lefkowitz. 1995. Mutational analysis of the pleckstrin homology domain of the β-adrenergic receptor kinase. *J. Biol. Chem.* 270:17000–17005.

Towbin, H., T. Staehelin, and J. Gordon. 1979. Electrophoretic transfer of proteins from polyacrylamide gels to nitrocellulose sheets: procedure and some applications. *Proc. Natl. Acad. Sci. USA.* 76:4350–4354.

Vega, M.A., B. Segui-Real, J. Alcalde Garcia, C. Calés, F. Rodriguez, J. Vandekerckhove, and I.V. Sandoval. 1991. Cloning, sequencing, and expression of a cDNA encoding rat LIMPII, a novel 74-kDa lysosomal membrane protein related to the surface adhesion protein CD36. *J. Biol. Chem.* 266:16818–16824.

Verheyen, E.M., and L. Cooley. 1994. Profilin mutations disrupt multiple actin-dependent processes during *Drosophila* development. *Development.* 120:

717–728.
von Heijne, G. 1986. Net N-C charge imbalance may be important for signal sequence function in bacteria. *J. Mol. Biol.* 192:287–290.
Wahlberg, J.M., and M. Spiess. 1997. Multiple determinants direct the orientation of signal-anchor proteins: the topogenic role of the hydrophobic signal domain. *J. Cell Biol.* 137:555–562.
Watanabe, N., P. Madaule, T. Reid, T. Ishizaki, G. Watanabe, A. Kakizuka, Y. Saito, K. Nakao, B.M. Jockusch, and S. Narumiya. 1997. p140mDia, a mammalian homolog of *Drosophila* diaphanous, is a target protein for Rho small GTPase and is a ligand for profilin. *EMBO (Eur. Mol. Biol. Organ.) J.* 16: 3044–3056.
Whitney, J.A., M. Gomez, D. Sheff, T.E. Kreis, and I. Mellman. 1995. Cytoplasmic coat proteins involved in endosome function. *Cell.* 83:703–713.
Williams, K.L., and P.C. Newell. 1976. A genetic study in the cellular slime mould *Dictyostelium discoideum* using complementation analysis. *Genetics.* 82:287–307.
Yanisch-Perron, C., J. Vieira, and J. Messing. 1985. Improved M13 phage cloning vectors and host strains: nucleotide sequences of the M13mp18 and pUC19 vectors. *Gene.* 33:103–119.
Yu, F.X., H.Q. Sun, P.A. Janmey, and H.L. Yin. 1992. Identification of a polyphosphoinositide-binding sequence in an actin monomer-binding domain of gelsolin. *J. Biol. Chem.* 267:14616–14621.